Astron. Astrophys. 319, 413–429 (1997)

ASTRONOMY
AND
ASTROPHYSICS

Broad band energy distribution of ROSAT detected quasars

I. Radio-loud objects⋆

W. Brinkmann, W. Yuan, and J. Siebert

Max-Planck-Institut für Extraterrestrische Physik, Giessenbachstrasse, D-85740 Garching, Germany

Received 25 January 1996 / Accepted 20 August 1996

Abstract. We present a sample of 654 radio quasars seen in the ROSAT All-Sky Survey and the ROSAT point source catalogue and study their broad band properties. The size of this list allows a statistically significant investigation of the soft X-ray properties of various subgroups distinguished by their radio properties. It is found that flat spectrum and steep spectrum quasars have slightly different X-ray properties which can be understood in the frame of a two component model for the emission: a beamed flat spectral component which is more dominant in flat radio spectrum objects and a steep more isotropic soft component. Combinations of these two components lead to the observed correlations of the X-ray spectral slope with the radio spectral properties, with the core dominance and radio loudness of the objects, and with redshift.

Various correlations exist between the radio, optical, and X-ray properties of the sources. Flat spectrum quasars are X-ray louder than steep spectrum objects, the X-ray loudness does not evolve with redshift, and the apparent dependence of α_{ox} on the optical luminosity seems to be due to biases inherent to the data. Simple proportionalities between the luminosities in the different wavelength bands appear to be inappropriate descriptions of the actual physical situation as they do not account for the varying contributions of the core and extended emission in the objects, i.e., the relative fraction of the beamed core to the unbeamed extended radio emission. Both components contribute in all energy bands but the physical processes governing these complex relations are not yet understood.

Finally, redshift dependencies and selection effects influence the correlations as well, leading to deviations from a simple linear relation between the measured quantities in many cases .

Key words: galaxies: active – quasars: general – radio continuum: galaxies – X-rays: galaxies

Send offprint requests to: W. Brinkmann

⋆ Table I is available in electronic form at the CDS via anonymous ftp 130.79.128.5 or http://cdsweb.u-strasbg.fr/abstract.html

1. Introduction

Quasars are the most luminous objects in the Universe and can thus be seen to highest redshifts. Therefore, they represent ideal probes for testing directly the physical conditions at large look back times. To do so, a detailed knowledge is required about the mechanisms of the quasar emission and about the cosmical evolution of the objects.

The most prominent quasars have been studied now for about 30 years over a broad energy band, from radio to γ-ray frequencies. However, nearby or extremely luminous objects might not be representative for the "typical quasar". Therefore, large samples of objects are required for a study of the general class properties of the quasars in order to overcome selection effects and observational biases.

Einstein IPC observations provided convincing evidence for a correlation of the X-ray emission with optical emission, for the presence of excess X-ray luminosity in radio-loud quasars, and for differences in the soft X-ray ($\sim$ 0.1 - 3.5 keV) spectral properties of radio-quiet and radio-loud quasars (cf. Avni & Tananbaum 1986, Canizares & White 1989, Wilkes et al. 1994). However, although the samples used were considerably larger than those of previous studies they hardly allowed to analyse the X-ray properties of various subgroups of quasars with statistically significant results. Especially for higher redshift quasars the results were ambiguous because of systematic uncertainties in the ensemble means.

The ROSAT instrument provides for the first time the opportunity to study a very large number of quasars in X-rays. More than $\sim$ 20000 AGN are expected to be detected in the ROSAT All-Sky Survey of which the majority remains to be optically identified in the future. A correlation of the ROSAT All-Sky Survey sources with existing catalogues yields a list of more than 900 quasars with many of them detected in X-rays for the first time.

In this paper we will present the broad band properties of the radio-loud objects; the discussion of the radio quiet quasars and their comparison with the radio-loud objects will be given in a consecutive paper (Yuan et al. 1996). We generally collected all quasars for which a published radio flux can be obtained from

the literature. However, some of the objects (in particular PG quasars) do not qualify as 'radio-loud' when the more restricted criterion for a quasar being radio-loud $log(f_{5\ GHz}/f_{2500\text{Å}}) > 1$ (or, using the corresponding K-corrected values, see Stocke et al. 1992) is taken. They are, therefore not used in any of the correlations but they are only mentioned for completeness and to demonstrate in a few occasions the transition to radio-quiet quasars.

In the next section we will present the data and give details of the derivation of the relevant parameters. In Sect. 3 we analyse the role of possible X-ray detection biases of the sample and in Sect. 4 we discuss the soft X-ray properties of the objects. We will then present their broad band spectral energy distribution (SED) and their evolution in Sects. 5 and 6. A general discussion of the sample follows in Sect. 7.

2. The data

We have compiled a sample of all quasars from the Véron-Cetty - Véron catalogue (1993, from now on VV93) detected by ROSAT in the ROSAT All-Sky Survey (Voges 1992), as targets of pointed observations, or as serendipitous sources from pointed observations as available publicly from the ROSAT point source catalogue (ROSAT-SRC, Voges et al. 1995).

Many of the radio-loud quasars presented here from the ROSAT All-Sky Survey (RASS) have been published recently from correlations of the RASS with the Molonglo 408 MHz Survey (Brinkmann et al. 1994, Paper I) and the Greenbank 5 GHz Survey (Brinkmann et al. 1995, Paper II). In total, these papers contain 360 objects, of which 346 are listed in VV93. This list is supplemented with 164 objects from the VV93 catalogue found additionally in more recent data from the ROSAT All-Sky Survey re-processing (SASS) or outside the spatial and flux limits of the two radio lists above, and a few new objects from recent publications.

The cross correlation of the VV93 radio quasars with the ROSAT-SRC, using a distance criterion between the optical and the X-ray source of $\Delta \leq 60''$, yields a list of 294 objects detected in pointed observations, many of them observed more than once. Amongst them, 100 objects are already included in Paper I and Paper II.

Taking into account the overlaps, the total number of ROSAT detected radio quasars from the above three sources is 654 objects, of which 360 were seen in the RASS only, 126 are only seen in pointed observations, and 168 were seen in both the RASS and pointed observations. It should be noted that the ROSAT All-Sky Survey detected sources form a well defined sample as the survey's limiting sensitivity is rather uniform (a few times 10^{-13} erg cm^{-2}s^{-1}) while the sources from pointed observations have vastly different exposures.

For objects which have been seen in both the ROSAT All-Sky Survey and pointed observations, we use the data from pointed observations for the determination of the spectral parameters, as Survey data suffer from much larger statistical errors due to the fact that the exposure in pointed observations is generally longer by more than an order of magnitude.

For 92 objects with sufficient numbers of source counts, spectral fits were made using a simple power law model with neutral absorption. For the rest, the power law indices (assuming Galactic or free absorption) were estimated using the two hardness ratios given by the SASS (Voges et al. 1992) by the method described in Paper I. We estimate the errors of the power law indices and the N_H values from the errors of the hardness ratios as described by Schartel (1995).

For 123 objects, no reasonable power law index Γ and absorption column density N_H could be obtained from the given hardness ratios, either due to the low number of source counts (with correspondingly large errors of the hardness ratios) or intrinsic deviations of the source spectra from simple power laws. For some objects published data exist in the literature; we use these results if they are of superior quality and mark them with their references.

82 objects have been observed in pointed observations more than once. For them, the mean values of Γ and N_H, as well as their corresponding 1σ errors are calculated, assuming that the source spectra do not vary between the different measurements. In fact, we found that in most cases the changes of the spectral properties are not significant and within the errors of the fitted parameters. The intensity variations of the sources will be discussed in Sect. 3.

The X-ray fluxes in the ROSAT (0.1-2.4 keV) band are calculated from the count rates using the energy to counts conversion factor (see Paper I) for power law spectra and Galactic absorption. For the power law index Γ we use the value obtained for the individual source if the estimated 1 σ error is $|\Delta\Gamma| \leq$ 0.5, and we take an average value $\langle\Gamma\rangle$ = 2.14 for the objects with low signal-to-noise ratios. It must be noted that slight differences in the power law slope do not affect the flux determination notably; the dominant parameter is the amount of absorbing matter in the line of sight.

In Table I we list the relevant information of all 654 quasars, starting with the IAU designation and the common name. Objects for which radio emission has been detected but which don't qualify as radio-loud according to the above mentioned flux criterion, are marked with a star. Then, following the J2000 positions, we list the redshift and optical magnitudes as found in VV93. In columns 5 and 6 we give the radio flux at 5 GHz as well as the radio spectral index α_r. The 5 GHz flux densities are taken from the 87GB radio survey (Paper II), from the NED data base, and from VV93. For most objects multi frequency radio data are available from NED which allows a good determination of the radio spectra. For objects with obvious power law spectra or objects with large scatter in the measured fluxes the spectral indices are determined by fitting a power law slope to the data. For objects showing a distinct non-power law spectral shape or when only few flux values are measured we calculated two point indices between 5 GHz and 1.4 GHz, if available.

In column 8 we list the (0.1 - 2.4 keV) unabsorbed X-ray flux obtained, as described above, with the assumption of a power law spectrum (i.e. the flux which would be measured without interstellar absoption). The given errors are the statistical errors from the count rates only. However, for sources with a small

number of total counts (mostly from the Survey) the systematic errors can be of the order of $\sim$ 30 % (see Paper I). For strong sources the assumed simple power law slope is often an inappropriate representation of the spectrum. In both cases the systematic uncertainties can be considerably larger than the purely statistical errors and the errors given in Table I should, therefore, be taken as lower limits. We then give the X-ray power law photon index with errors obtained under the assumption of Galactic absorption, an indication whether the object was seen in the Survey only (S), in a pointed observation (P), or in both (SP). The last entry gives a reference to other published results.

From the point of view of a radio classification the list contains a total of 297 flat spectrum and 201 steep spectrum quasars. We considered sources with $\alpha_r > -0.5$ as flat spectrum objects and as steep spectrum sources those with $\alpha_r < -0.5$. 24 objects were classified as 'Gigahertz Peaked Spectrum' (GPS) and 12 as 'Compact Steep Spectrum' (CSS) sources. For the rest of the objects the radio information is insufficient for a classification, unclear, or the objects are not radio-loud.

Many of the radio-loud objects in the VV93 compilation are not primarily radio detected quasars but have been discovered in other wavelength bands (X-rays, optical) and subsequently found to be radio emitters as well. To avoid any possible detection biases which might influence the correlations of the broad band properties of the sources we will restrict the statistical analyses to objects only, which were first detected in well defined radio surveys. These are, ordered according to the number of objects entering our list, the Kühr 1Jy sample (Kühr et al. 1981a), the Parkes Survey (Bolton et al. 1979), the B2 catalogue (Grueff & Vigotti 1975), the 3CR sample (Laing, Riley & Longair 1983), the Molonglo Reference Catalogue (Large et al. 1981), the 4C list (Gower et al. 1967), and the S4 (Pauliny-Toth et al. 1978) and S5 catalogues (Kühr et al. 1981b). This gives a total of 465 sources radio detected in well defined samples at different frequencies from large regions of the sky. The reduced sample is still large enough to have a sufficient number of objects in any subclass of radio quasars for a high quality statistical analysis.

3. Non - detections, variability

Before discussing the ROSAT detected objects in more detail we want to compare the sample with those objects, for which no X-ray data are available.

There are 1033 radio detected objects in the VV93 catalogue which were not seen in the ROSAT All-Sky Survey . 126 of these objects were later discovered in deeper pointed observations. A comparison of the properties of these less X-ray loud catalogued sources with those detected in the ROSAT All-Sky Survey can give valuable information about the reasons for a source not to be detected in X-rays as well as on the inherent biases and uncertainties of the selected sample.

In Fig. 1 we plot the histogram of the count rates of all sources detected in the RASS and, as shaded area, of those not seen in the RASS but in pointed observations only. It appears

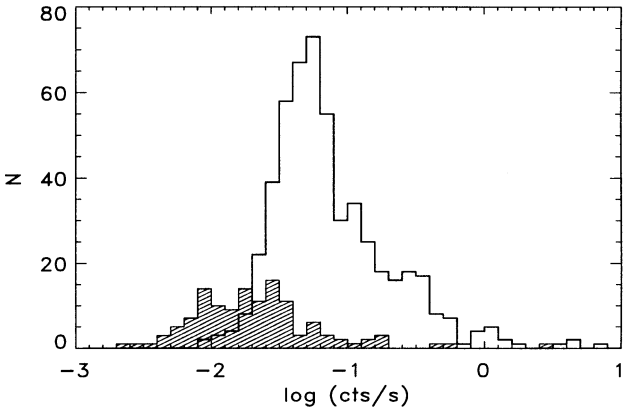

Fig. 1. Histogram of the count rates of objects seen in the RASS (open line) and those not detected in the Survey but in pointed observations.

that the non detections are in general below or close to the sensitivity limit of the Survey. We checked the RASS data of all not detected sources with count rates greater than 0.025 counts s^{-1} in pointed observations. A small fraction of the objects either falls onto the strip boundaries in the SASS processing where the detection efficiency is reduced, or they are in regions of exceptionally low Survey exposure, or in regions with enhanced diffuse emission. The majority of the objects had a rather low signal-to-noise ratio in the Survey and was thus not regarded as a statistically significant detection by the SASS. Only a small number of quasars (of the order of $\leq$ 10%) might have been missed due to their intrinsic variability. Thus we have to conclude that most of the 'non-detections' are sources with soft X-ray fluxes below the Survey's limiting sensitivity.

More than 82 quasars have been observed repeatedly in pointed observations and thus provide a good test sample for an evaluation of the variability of the sources. In Fig. 2 we plot a histogram of the maximal variability of the objects, i.e., the ratio of the higher count rate divided by the lower count rate. If a source has been observed more than twice only the maximum and the minimum values have been used.

Fig. 2 clearly shows that a large fraction of the quasar population is variable, however mostly by less than a factor of two. For weak sources low variability cannot be distinguished from statistical fluctuations. Only 3 objects vary by more than a factor of 5: S4 1050+54 by a factor of $>$ 9, MS 09584+6913 by more than a factor of 7, and 1E 1640+401 by a factor $\sim$ 5.6. Unfortunately, as most of the individual observations on a source have been performed in different ROSAT pointed observation periods, i.e., at least half a year apart, we cannot make any reliable statistical estimates about a relation between the time scale and the amplitude of the variability of a source.

3.1. Detection biases

The ROSAT All-Sky Survey has a relatively uniform limiting sensitivity of a few $\times$ 10^{-13} erg cm^{-2} $s^{-1}$with the exact value depending slightly on the amount of intervening Galactic ab-

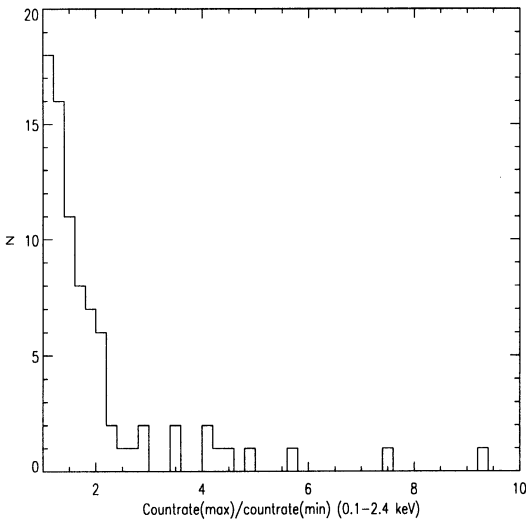

Fig. 2. Histogram of the variability of quasars seen more than once in pointed observations.

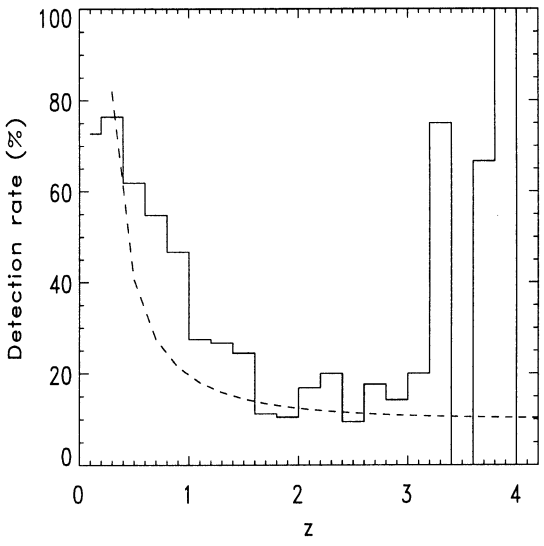

Fig. 3. Detection probability in percent of radio selected quasars in the RASS as a function of redshift.

sorption, on the exact shape of the X-ray spectrum of the quasar, and on the local Survey exposure.

In Fig. 3 we show the detection rate in percent of the quasars as function of redshift, i.e., the number of objects from the radio selected sample detected in the RASS in a redshift bin divided by the total number of catalogued radio-loud quasars for that redshift. The dashed line represents a curve $\sim (1+z)^{2.8}/D_L^2$, where $D_L(z)$ is the luminosity distance (Schmidt & Green 1986) assuming a Friedman cosmology with $H_0 = 50$ km s^{-1} Mpc^{-1} and $q_0 = 0.5$[1]. The redshift term accounts approximately for the quasars' luminosity evolution (Boyle et al. (1993) derive a value

[1] These values are used throughout the paper.

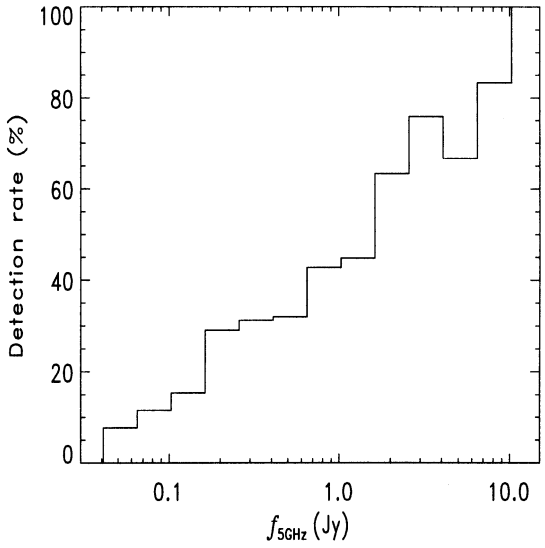

Fig. 4. Detection probability in percent of quasars in the RASS as function of the 5 GHz radio flux.

of $k = 2.8 \pm 0.1$ for the X-ray luminosity function, however, for a $q_0 = 0$ universe). The detection rate roughly follows this simple law, with positive deviations around $z \sim 1$ (as noted for ROSAT detections of quasars in general, Boyle et al. 1993) and large scatter at high redshifts. Details like luminosity K-corrections and N_H variations seem to play only a minor role.

The total average detection rate of all radio-loud quasars in the RASS is about 33.2%, markedly higher than the $\sim 5.5\%$ of radio-quiet objects (Yuan et al. 1996) and at highest redshifts more than 50% of the catalogued objects are detected. This high detection rate indicates that the currently known high z quasars are 'special' in a certain sense.

As the sample is drawn from existing flux limited radio surveys, changes of the detection probability as a function of radio flux density give insight into the relative strengths of the X-ray and radio emission of the objects.

In Fig. 4 we show the detection probability (in percent) as function of the 5 GHz radio flux density. The probability increases from about 10% at low radio fluxes to more than 75% at the highest radio fluxes. It should be noted that, at even lower radio fluxes not shown here this value increases again due to the inclusion of X-ray loud Seyfert I type QSOs like the PG sample which are nearby objects but, as mentioned above, don't qualify properly as radio-loud quasars.

The decrease of the X-ray detection rate with radio flux clearly shows the X-ray detection bias caused by the sensitivity limit of the RASS. The radio surveys are thus, relative to the X-ray observations, more sensitive. Additional changes of the source population or luminosity dependent variations of intrinsic source properties cannot be ruled out either.

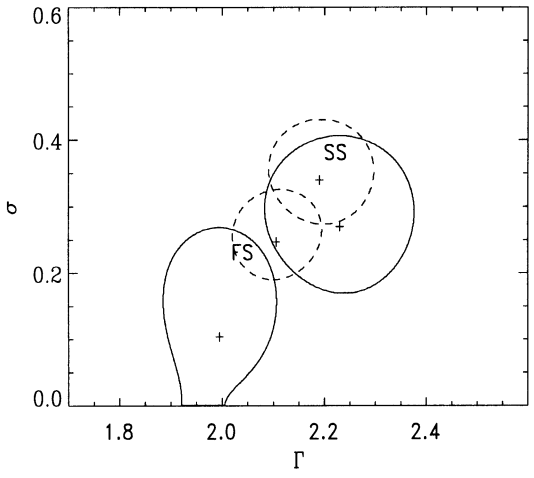

Fig. 5. Best-fit mean spectral index and Gaussian standard deviation for power law fits to flat (FS) and steep radio spectrum (SS) sources assuming Galactic absorption (dashed curves) and free-fit absorption (full curves). Contours correspond to 90% confidence levels.

4. The X-ray properties

From the Einstein IPC data it is known that radio-loud and radio-quiet quasars show different power law slopes ($\Gamma_{IPC,rl} \sim 1.5$, $\Gamma_{IPC,rq} \sim 2.0$; Wilkes & Elvis 1987, Canizares & White 1989, Brunner et al. 1989, Shastri et al. 1993). Further, various correlations of the photon index with other source properties have been claimed for subclasses of objects, for example with core dominance (Wilkes 1994, and references therein), with redshift (Schartel et al. 1992), or with radio spectral index (Brunner 1992). As the current sample is considerably larger than all samples used before we are able to draw statistically more reliable conclusions on the claimed correlations - however, in the somewhat softer (0.1 - 2.4 keV) ROSAT PSPC energy band.

4.1. The average photon index Γ

The results of a maximum-likelihood analysis for the distribution of power law slopes for flat spectrum and for steep spectrum quasars is given in Fig. 5 (for details of the analysis see Maccacaro et al. 1988, Worrall & Wilkes 1990). To minimize evolutionary effects, we restricted the redshift range to $z \leq 1.0$ which resulted in a sample of 102 flat and 104 steep spectrum sources for which a spectral index is available for fits with free N_H and for fits assuming Galactic N_H. A discussion of the redshift dependence of the power law slopes will be given in the next section.

In Fig. 5 the contours correspond to 90% confidence levels. The fits are done assuming Galactic absorption only (dashed lines) or the absorbing column density is left free in the fit (full lines).

Evidently, flat spectrum quasars show a flatter X-ray power law spectrum than steep radio spectrum objects. Remarkable is the fact that in flat spectrum sources, leaving the amount of absorption as a free parameter, the dispersion of the spectral indices is compatible with zero. I.e., all flat spectrum quasars have a very similar soft X-ray power law slope. Forcing the absorption to the Galactic value increases the dispersion considerably demonstrating that a noticeable number of objects show absorption deviating from the Galactic value or have spectra not following a simple power law. Interestingly, in the case of the steep spectrum sources the two distributions are very similar. This implies that either steep spectrum objects form an intrinsically inhomogeneous group where the physical conditions determining the X-ray spectra are differing from object to object, or the X-ray emitting region is intrinsically absorbed in many of the objects. This might be caused by orientation dependent absorption in a molecular torus or by conditions similar to those found in CSS, where it has been proposed that the sources are being inhibited from growing to larger dimensions by unusual conditions of the interstellar medium (Fanti & Fanti 1994).

We have analyzed separately the small group of objects classified as 'Compact Steep Spectrum' (CSS, Fanti et al. 1990) and as 'Gigahertz Peaked Spectrum' sources (GPS, O'Dea et al. 1991). Interestingly, the GPS sources have a flatter photon index $< \Gamma >$ = 1.86 (for N_H free) and $< \Gamma >$ = 1.50 for Galactic N_H, and a dispersion σ which is consistent with zero for the fits with free N_H. For the CSS sources we find $< \Gamma >$ = 1.88 (N_H free) and $< \Gamma >$ =1.99 (Galactic N_H), both with large dispersion $\sigma \sim 0.48$.

It is not clear whether this dichotomy of the X-ray spectral slopes is a 'fixed' property of the flat spectrum and steep spectrum classes or whether there is a continuous mutual dependence of the two spectral indices. Taking the power law indices obtained with the assumption of fixed Galactic absorption and using only objects with errors in the indices $|\Delta\Gamma| \leq 2$ a linear regression analysis (Draper & Smith 1966) gives for a fit of the X-ray photon index versus radio spectral index $\Gamma = (1.95 \pm 0.03) - (0.22 \pm 0.06) \times \alpha_r$ with a non-parametric Spearman rank correlation coefficient R_{sp} = -0.23 for 264 d.o.f., at a probability level of $P_r = 1.5 \times 10^{-4}$. P_r is the probability that the observed correlation occurs by chance for uncorrelated data sets (Press et al. 1986). All errors given are 68% confidence limits (1 σ). It should be noted that we obtain here and in the following identical results (inside the mutual 1 σ errors) for fits with free absorption. The regression curve is given as dashed line on the data in Fig. 6. Throughout the paper the following symbols will be used for the different object classes: $\circ$: steep spectrum objects, $\bullet$: flat spectrum objects, $\triangle$: CSS objects, $\square$: GPS objects.

We tested this general trend against regression fits of the two classes of objects separately. The regression line for the subsample of 114 steep spectrum objects is given by $\Gamma = (1.74 \pm 0.19) - (0.51 \pm 0.23) \times \alpha_r$, that for the 150 flat spectrum objects $\Gamma = (1.94 \pm 0.04) + (0.02 \pm 0.13) \times \alpha_r$. While for flat spectrum sources the Spearman rank correlation analysis gave a probability for no correlation of $P_r \sim 0.87$, this hypothesis can be ruled out with $\sim 98.7\%$ confidence for the steep spectrum objects. For flat spectrum sources the assumption that the data set can be described by the 'general' slope of $\beta_{tot} = -0.22$ can

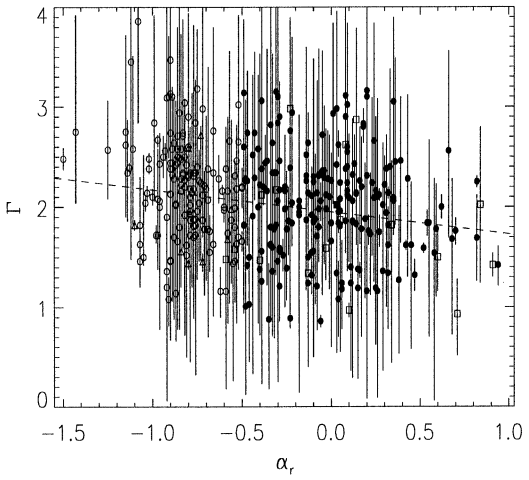

Fig. 6. X-ray photon index Γ (assuming fixed Galactic absorption) as a function of the radio spectral index α_r. ○ : steep spectrum objects, ● : flat spectrum objects, △ : CSS objects, □ : GPS objects.

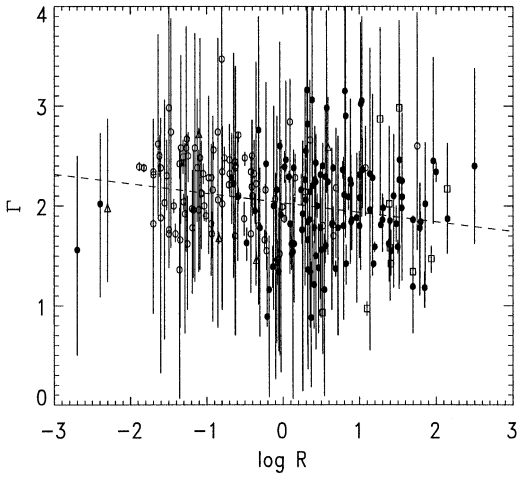

Fig. 7. X-ray photon index Γ as a function of the core dominance $R = S_{core}/S_{ext}$. Symbols as in Fig. 6.

be ruled out with almost 95 % confidence, for steep spectrum objects with ∼ 79% only.

This result strongly suggests that flat spectrum and steep spectrum sources are from an X-ray point of view intrinsically different types of objects, but so far the physically relevant parameter responsible for this difference has not been found. If these differences can be related to orientation effects the changes of the emission characteristics must occur rather abruptly as there seem to be no smooth transitions of the X-ray properties between the different sub-classes or the radio spectral index α_r is not an appropriate measure of the quasar's intrinsic properties.

4.2. Core dominance

The X-ray slopes of core and lobe-dominated radio-loud quasars were found to be different (Boroson 1989, Wilkes & Elvis 1987, Canizares & White 1989, Brunner et al. 1992, Shastri et al. 1993) which was interpreted as a slope continuously flattening with core dominance R = S_c / S_{ext}. Here S_c and S_{ext} are the core and extended flux densities at 5GHz, respectively, K-corrected assuming $\alpha_c = 0$ and $\alpha_{ext} = -1.0$. The core fluxes were obtained from the literature and from recent VLA observations of radio-loud ROSAT sources (Laurent-Muehleisen et al. 1996).

A plot of the photon index Γ versus core dominance actually shows a correlation between these two quantities with a Spearman rank coefficient $R_{sp} = -0.27$ and a probability level $P_r < 8 \times 10^{-4}$.

The common explanation for the flattening of the X-ray spectrum with core dominance would be that the beaming angle influences the slope of the spectrum. However, Fig. 7 indicates that this result can also be interpreted as a correlation between radio slope α_r and X-ray photon index Γ: the flatter X-ray spectrum sources are predominantly found at higher core dominance, a quantity which can be connected directly to flatter radio spectra. Similar correlations were noticed previously, for example by Kembhavi et al. (1986) and at higher X-ray energies by Williams et al. (1992) using Ginga data. However, a partial Spearman rank correlation analysis did not reveal which of the underlying parameters is fundamentally correlated with Γ.

4.3. Radio loudness

The use of the extended flux density for normalizing the boosted flux of the core introduces considerable scatter in the determination of the beaming angle as the emission from the radio lobes depends strongly on the interaction of the jet with the environment. Therefore, the ratio of radio core to optical continuum luminosity, i.e., the radio loudness, has been proposed as a more suitable core dominance parameter (Wills & Brotherton 1995). Indeed, the plot of the core dominance R versus radio loudness R_L for our sample shows a relatively well defined correlation over a large parameter range - with some scatter. From Ginga observations Williams et al. (1992) find a possible correlation between the X-ray medium energy (2 - 10 keV) spectral index and radio loudness at the 90% level, however for a rather small sample of radio-loud quasars.

In Fig. 8 we show the photon index Γ as function of radio loudness, again for flat spectrum and steep spectrum sources. There is certainly a trend of decreasing Γ with increasing radio loudness. However, this is partly masked by the effect that steep spectrum objects are predominantly found at lower radio loudness, flat spectrum sources at higher radio loudness. The combined two classes of objects show a trend of the form $\Gamma \sim \alpha \times log(L_{core}/L_{opt})$, with $\alpha = -0.14 \pm 0.04$ with a Spearman rank coefficient of $R_{sp} = -0.34$ and a probability level $P_r = 2 \times 10^{-5}$.

Interestingly, comparing Fig. 7 and Fig. 8 we find that the trends of Γ versus core dominance R or versus radio loudness R_L are similar, except at high values of R and R_L where Γ seem to decrease with R_L but to increase with R. Similar deviations from a linear relation at higher values of these parameters are

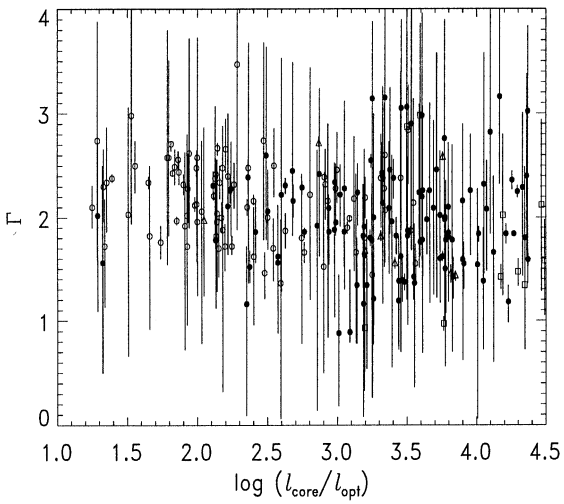

Fig. 8. X-ray power law photon index Γ as a function of the radio loudness R_L. Symbols have the usual meaning.

seen as well in the plot R versus R_L. This is not unexpected as the discussion (chapter 5) of the luminosity correlations clearly shows that the optical luminosity is correlated with the (beamed) X-ray luminosity indicating that the optical emission is, at least partly, beamed as well (Baker et al. 1994). Thus its use as an orientation indicator based on an assumed isotropy of the optical emission seems to be questionable.

4.4. Redshift dependence

Quasars are seen over a large range of cosmological distances and, correspondingly, the observed spectral energy band transforms into different intrinsic energy bands in the source frames. Secondly, quasar luminosity functions show evolution (cf. Ciliegi et al. 1995, Boyle et al. 1993) and, therefore, a cosmological evolution of the quasars spectral properties cannot be ruled out either.

Canizares & White (1989) find no evidence for a dependence of the power law slope on z for quasars observed with the IPC. In the softer ROSAT energy band Schartel et al. (1992) report a flattening of the power law spectra with redshift while Bechtold et al. (1994) claim similar slopes for high and low redshift radio-loud quasars, however, with substantial intrinsic absorption for objects at high z.

In Fig. 9 we show the photon indices (assuming Galactic absorption, again) as a function of redshift for flat spectrum (upper panel) and for steep spectrum quasars. Again, we have excluded the objects with large errors in the photon index ($|\Delta\Gamma| > 1$) from the analysis and sources found in regions of exceptionally high Galactic absorption ($N_H \geq 10^{21}$ cm^{-2}) as it cannot be ruled out that the fitted values of the spectral slopes are affected by the correspondingly narrow remaining energy window. We further excluded 3 objects with very high photon statistics which show definite deviations from a simple power law. Finally, for 8 objects with clear indications of additional intrinsic absorption we used the free - fit values for the power law slopes.

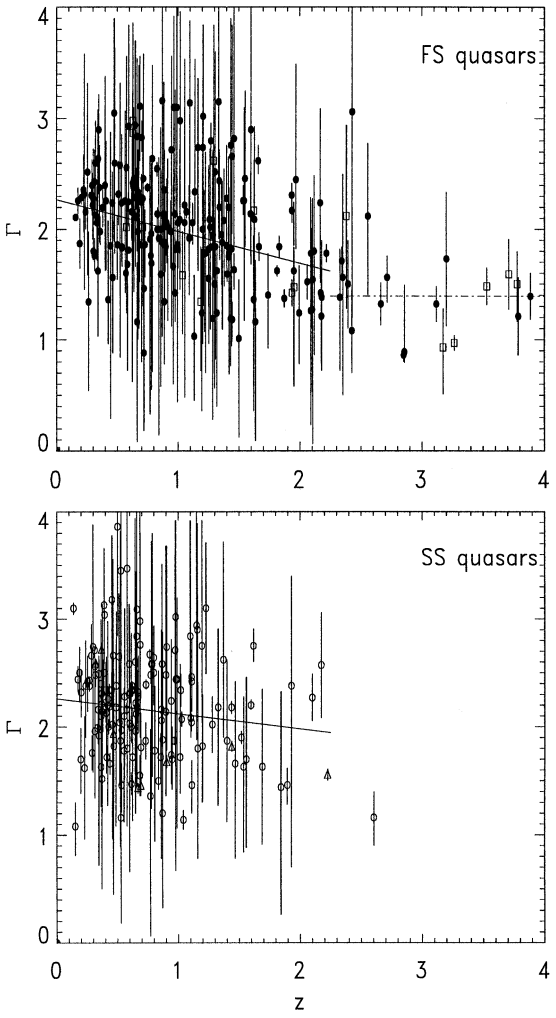

Fig. 9. X-ray photon index Γ as a function of redshift z for flat spectrum and GPS (top) and steep spectrum and CSS (bottom) quasars. For clarity only data points with $|\Delta\Gamma| \leq 2.0$ are plotted and the symbols have the usual meaning. The fitted linear regression curves are given.

For flat spectrum quasars a single regression curve gives an acceptable fit (Spearman rank probability level $P_r \sim 3\times10^{-10}$). However, the fit of this total slope for the subset of quasars at $z >$ 2 alone is unacceptable and the data are indicative for a redshift dependent broken line. Fitting two straight lines results in a z-dependent correlation of the form $\Gamma = (2.27 \pm 0.07) - (0.29 \pm 0.06) \times z$ for redshifts $z \leq 2.25$ and a redshift independent component with $\Gamma = 1.48 \pm 0.07$ for $z > 2$. The regression analysis for the subsample of steep spectrum objects (excluding 12 CSS objects) gives $\Gamma = (2.29 \pm 0.08) - (0.19 \pm 0.11) \times z$, using objects with $z \leq 1.75$ for the fit. For flat spectrum sources the hypothesis of 'no correlation' can be ruled out with almost 100% confidence, for steep spectrum objects with 91%.

The break in the fitted line of the power law index around z $\sim$ 2 for the flat spectrum quasars is probably not related to evolutionary effects seen in the luminosity function of X-ray selected quasars (Boyle et al. 1993). The changes are more likely

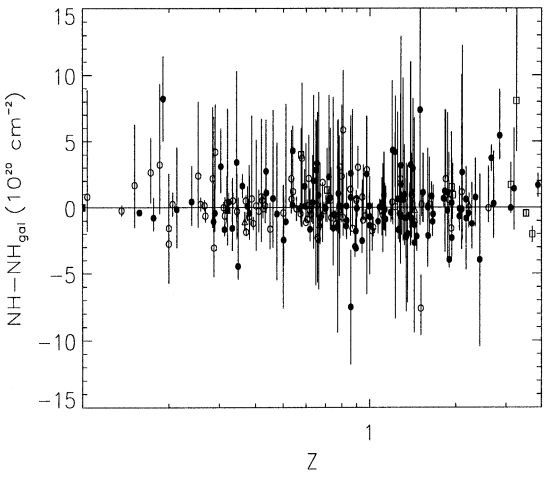

Fig. 10. The difference between the fitted absorption and the value of Galactic absorption to the source (in units of 10^{20} cm^{-2}) as a function of redshift z.

caused by the fact that with increasing redshift the soft X-ray excess 'moves out' of the PSPC's energy window - modified by the different amounts of Galactic absorption towards the sources. The photon index thus approaches the average redshift independent value found in the higher energy band (E $\geq$ 2 keV) by EXOSAT (Lawson et al. 1992), Ginga (Williams et al. 1992), and ASCA (Siebert et al. 1996, Cappi et al. 1996) for high redshift quasars.

Finally, we investigated the possible dependence of excess absorption in the fitted spectra with redshift. Absorption intrinsic to the quasars themselves could yield information about their evolution and their local environments; excess absorption along the line of sight places limits on a hot diffuse intergalactic medium and on physical conditions in damped Lyman-α absorbers (Elvis 1994).

In Fig. 10 we plot, for all objects, the differences between the fitted absorption and the Galactic absorption towards the sources in units of 10^{20} cm^{-2} as a function of redshift. A few objects which evidently show excess absorption $N_H - N_{H,gal} > 1.5 \times 10^{21}$ cm^{-2} and some objects with errors larger than $|\Delta N_H| > 10^{21}$ cm^{-2} are outside of the plot boundaries.

For most of the objects the N_H values are compatible with the Galactic values within their 1 σ errors. We do not see a statistically significant systematic trend with z and the results of a regression analysis (applying different $|\Delta N_H|$ - cuts to avoid 'outliers') are inconclusive. The differences found for individual sources can be related to intrinsic absorption in these objects or to the fact that a single power law is an inappropriate representation for the soft X-ray spectrum. Interestingly, there seems to be a higher fraction of quasars with intrinsic absorption at high redshifts an effect only found for radio-loud quasars (Elvis 1996). The GPS objects seem to have a tendency to show (on average) absorption in excess of the Galactic values, for CSS objects we find the opposite behavior. However, these two samples are too small for statistically reliable conclusions.

5. The spectral energy distribution

5.1. Luminosity - redshift relation

The conversion of the observed flux into a luminosity involves, besides the distance term, a luminosity K-correction (Schmidt & Green 1986) given as

$$C(z) = (1+z)^{-(1+\alpha)},$$

where α is the energy index of the assumed power law continuum spectrum, S(E) $\sim E^{\alpha}$.

In the soft X-ray band the spectral slope itself is a function of redshift (see Fig. 9). In the optical band there are indications that the continuum slope is a function of the core dominance R (Baker & Hunstead 1995). Further, an additional correction taking into account the fact that the quasar spectrum is not strictly a power law, but is affected by emission lines and by the Lyman α forest depleting the continuum to the blue of Lyα (VV 93) should be considered.

For a redshift of z = 2, using for X-rays the range of photon indices as discussed in Sect. 4.4 and for the optical band the different values given by Baker & Hunstead (1995), the K-correction term amounts to approximately $0.57 \leq C_{z=2} \leq 1.5$. This means that an inappropriate knowledge of the spectral properties of a source at higher redshifts can lead to uncertainties in the calculated luminosity of a factor of ~ 3.

In the following we will use for the K-correction in the radio band the power law index determined as above for each individual source. In the optical we take a continuum slope of α = 0.5 with line corrections as given by Avni & Tananbaum (1986), and in the X-ray range the z-dependent average power law indices as determined in Sect. 4.4.

In Fig. 11 we show the K-corrected (0.1 - 2.4 keV) luminosities of our sample as a function of redshift. The different object classes are indicated by the usual symbols. For illustrative purposes we include (full curve) the typical Survey detection limit for a source with an X-ray flux of 4×10^{-13} erg cm^{-2} s^{-1}, ignoring the effects of Galactic absorption. The luminosity K-correction for this curve was done as well with a redshift dependent photon index as determined in Sect. 4.4. It can be seen that many sources have luminosities definitely below the Survey flux limit and are thus only detected in pointed observations. At higher redshifts only flat spectrum and GPS objects are found. A relatively high fraction of very luminous objects can be seen around z$\sim$ 2, in accordance with current schemes of quasar luminosity evolution. The two brightest sources near z = 2 are PKS 2149-306 and the γ - bright quasar S5 0836+710.

5.2. Luminosity - luminosity correlations

Previous studies of radio-loud quasars (Avni & Tananbaum 1986, Browne & Murphy 1987, Kembhavi et al. 1986, Worrall et al. 1987, Wilkes et al. 1994, Paper I, II) find a non-linear relationship between the X-ray and optical luminosities of the form $L_x \sim L_o^{\beta}, \beta \neq 1$. A knowledge of the exact form of this relation is required to relate the quasar statistics (evolution, luminosity function) in the two wave-bands and to understand the

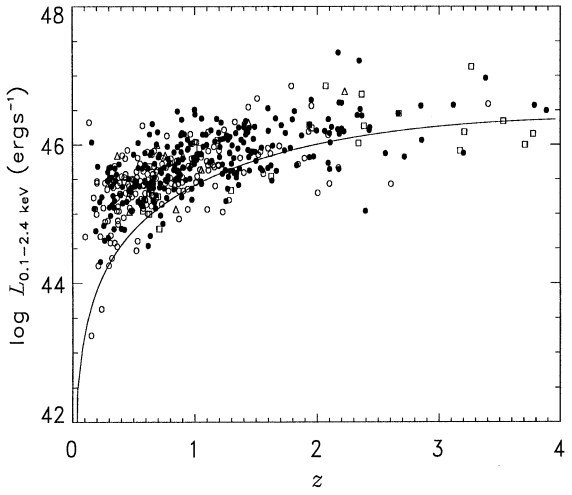

Fig. 11. (0.1-2.4 keV) soft X-ray luminosity as a function of the redshift z. Different object classes are indicated by the usual symbols. Plus signs (+) indicate sources without known radio slopes. The full curve represents the luminosity of a source at a Survey flux limit of 4×10^{-13} erg cm^{-2} s^{-1}, K-corrected with a redshift dependent photon index.

quasar's broad band emission. The fitted slopes of the regression curves in the individual papers differ markedly and they further seem to depend on the sample under consideration and on the method employed for the determination of the correlation (see the discussion by Padovani 1992, Franceschini et al. 1994, and La Franca et al. 1995).

Most of the data used previously were from Einstein IPC observations with relatively low quality spectral information and a major source of the statistical uncertainties were the generally rather small samples of different object classes. In both respects the ROSAT data provide a substantial improvement and considering the importance of obtaining an exact value of the slope of the luminosity correlations we test different mathematical correlation analysis methods to understand their limitations.

For this we used from the total data set a 'test sample' of 278 flat spectrum sources with $29.6 \leq \log(l_o) \leq 31.7$. When errors were considered in the analysis we took Δm = 0.2 mag for the optical data , and the statistical errors from Table 1 for the X-ray fluxes. In Table 2 we present the results of various methods for the determination of the slope of a correlation of the form $\log(l_x) \sim \beta \log(l_o)$.

In the first two tests we employed an unweighted ordinary least square regression which can be found in standard analysis packages like IDL or Numerical Recipes. Taking the x-coordinate (optical luminosity) as independent and the X-ray luminosity as dependent variable, both without errors, we obtain a slope similar to that found in Papers I, II and others. However, reversing dependent and independent variables the fitted slope is not the inverse of the previous one. This indicates that there is no 'physical' separation into an 'independent' coordinate and a coordinate dependent 'variable', and as a more 'reasonable slope' the bi-section of these two slope should be used (Feigelson & Babu 1992). Including the errors of the X-ray luminosity into the analysis results in a similar slope (inside the 1 σ errors) as without errors. This means that our sample is large enough not to be dominated by statistical errors and that the data points are statistically independent. The method of orthogonal distance regression (ODRPACK, Boggs et al. 1990) gives a slope around β = 1.0, if errors in both variables are considered. Finally, we tried a generalized orthogonal regression proposed by Fasano & Vio (1988, FV) which takes into account both measurement errors and intrinsic variances (i.e., scatter around the regression line) usually unaccounted for by the observational uncertainties. Setting the intrinsic variance $\sigma \rightarrow 0$ we obtain a slope consistent with the corresponding ODR result. With free fitted variance the slope gets even steeper than unity with a variance considerably different from zero. This implies that there is already some intrinsic scatter in the correlation of the luminosities, not accounted for in standard regression analysis techniques.

Thus, considering the relatively large uncertainties inherent in the data, an ODR regression analysis, taking into account errors in both variables is most appropriate, at least for luminosity - luminosity correlations. Therefore, we will employ this method in the following sections for the study of these correlations.

Table 2. Regression analysis for test sample of flat spectrum sources

Method	error	β	Remarks[a)]
OLS (y|x)[b)]	no error	0.75±0.05	IDL/Num.Rec.
OLS (x|y)	no error	0.64±0.04	IDL/Num.Res.
OLS (y|x)	y error	0.69±0.28	IDL
ODR[c)]	no error	1.12±0.05	ODRPACK
ODR	y error	0.76±0.05	ODRPACK
ODR	x,y error	1.02±0.05	ODRPACK
ODR	x,y error	0.98±0.12	FV, σ = 0.0
ODR	x,y error	1.19±0.05	FV, $\sigma = 0.19 \pm 0.02$

[a)] source of code used
[b)] ordinary least squares solution
[c)] orthogonal distance regression

5.3. l_x- l_o- correlation

Fig. 12 shows the correlation of the monochromatic 2 keV X-ray luminosity with the monochromatic 2500 Å optical luminosity. An ODR regression analysis as described above gives a linear fit log (l_x) = (0.86 ± 0.11)· (log(l_o) - 30.5) + (27.33±0.07) for the flat spectrum sources and for the steep spectrum sources log (l_x) = (0.79 ± 0.16)· (log(l_o) - 30.5) + (27.08± 0.08). The Spearman rank correlation coefficients are R_{sp} = 0.71 for flat spectrum and R_{sp} = 0.61 for steep spectrum objects, respectively. For both cases the probability levels are $P_r < 10^{-18}$. The different values for the regression constant imply that for a given optical luminosity flat spectrum quasars are about 50% X-ray brighter than steep spectrum quasars.

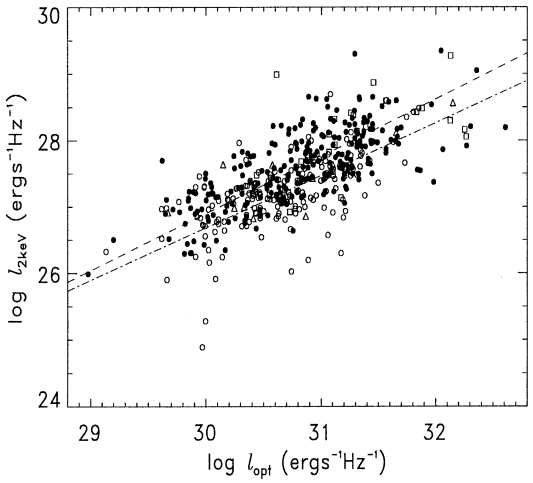

Fig. 12. The monochromatic X-ray luminosity as a function of the optical 2500 Å luminosity. Symbols as in Fig. 6. The linear regression lines are plotted for flat spectrum quasars (dashed line) and steep spectrum quasars (dash-dotted line).

Table 3. Redshift dependent regression analysis for flat spectrum sources

Redshift range	N($< z$)	slope
z $\leq$ 0.5	37	0.92$\pm$ 0.42
z $\leq$ 1.0	126	0.65$\pm$ 0.19
z $\leq$ 1.5	192	0.69$\pm$ 0.15
z $\leq$ 2.0	213	0.76$\pm$ 0.14
z $\leq$ 2.5	232	0.87$\pm$ 0.13
z $\leq$ 4.0	240	0.94$\pm$ 0.13

Very similar slopes for the l_x- $l_o$relation have been found for the optically selected LBQS sample (Green et al. 1995), for an X-ray selected sample of ROSAT and EMSS sources (Boyle et al. 1993), as well as in many earlier studies (e.g. Wilkes et al. 1994). This seems to indicate that the high energy emission in quasars is of similar origin, independent of the quasar's radio properties.

Of particular interest is the sample of 252 flat spectrum objects, which show a definite flattening of the correlation at high optical luminosities. Using a broken slope for the regression line (break luminosity at log(l_o) $\sim$ 31.5) the two slopes turn out to be $\beta_{FS,h}$ = 0.96 $\pm$ 0.13 and $\beta_{FS,l}$ = 0.05 $\pm$ 0.7, respectively. This flattening is obviously a luminosity, not a redshift effect, as an inspection of the optically very bright objects shows that they are found over the whole redshift range.

Ignoring the 10 optically brightest and 2 optically faintest objects, i.e., taking a truncated sample of 240 flat spectrum sources (again with 29.6 $\leq$ log(l_o) $\leq$ 31.7) and performing a regression analysis for restricted redshift ranges we find a steepening of the regression slope with increasing redshift (Table 3).

Whether this steepening is a genuine physical effect needs to be investigated as the influence of observational biases and redshift dependent selection effects on the correlations are not fully understood at present. Changes of the luminosity K-correction for the optical luminosities by varying the spectral slopes (0.3 $< \alpha_o <$ 0.75) lead to slightly different slopes in the various redshift bins but the general trend of steepening with redshift remains. Worrall et al. (1987) claim that the inclusion of a redshift term in the analysis does not change the correlations noticeably. These findings have been criticized by Padovani (1992), noting that the samples used were inhomogeneous and incomplete.

The possible introduction of detection biases through distance (redshift) effects does not justify the search for correlations amongst the corresponding flux densities. If there exist a relationship between the intrinsic luminosities, for example of the form $L_x \sim L_o^b$, a correlation between the flux densities might disappear unless b = 1, as shown by Feigelson & Berg (1983) and Kembhavi et al. (1986). To assess quantitatively the extent of a spurious correlation introduced by distance effects the partial linear correlation coefficient $R_{rx,z}$ (e.g. Hald 1952) can be used. We determined the partial correlation coefficients $R_{rx,z}$ with the effect of redshift (i.e. luminosity distance) eliminated for all luminosity - luminosity correlations studied in this paper and found that in all cases the influence of a luminosity - redshift dependence on the correlations can be ruled out with high probability ($P_r < 10^{-6}$).

Luminosity correlations can suffer biases if upper limits are not included in the analysis. We used the tools of the survival analysis package ASURV Rev 1.3 (LaValley et al. 1992) and tested the effects of including the $\sim$ 890 upper limits in the regression analysis. Remembering, that no measurement errors are considered in that analysis the regression slope gets only slightly flatter when the upper limits are included. For example, the slope of the l_x- l_o regression changes from 0.74 (no upper limits) to 0.70 with upper limits. These changes are smaller than the differences found between various regression analysis methods.

Finally, there might be observational biases as X-ray flux limited observations will preferentially select objects with larger values of l_x/l_o as discussed by Cheng et al. (1984).

Summarizing, we can say that a simple correlation $l_x \sim l_o$ as favored by some evolutionary considerations cannot be ruled out, but the various subsamples show different slopes, redshift dependencies, changes in the slopes as a function of the sample parameters and, over all, possibly a non negligible intrinsic dispersion of the source properties. These effects can be imposed by selection and detection biases or by intrinsic, physically different source properties not yet accounted for. Thus, although we have at hand the by far largest sample of X-ray detected radio-loud quasars the conclusions we draw might be valid only for the objects we have 'seen'. In particular, there might be a whole population of 'X-ray quiet' radio-loud quasars, as already discussed in Paper I.

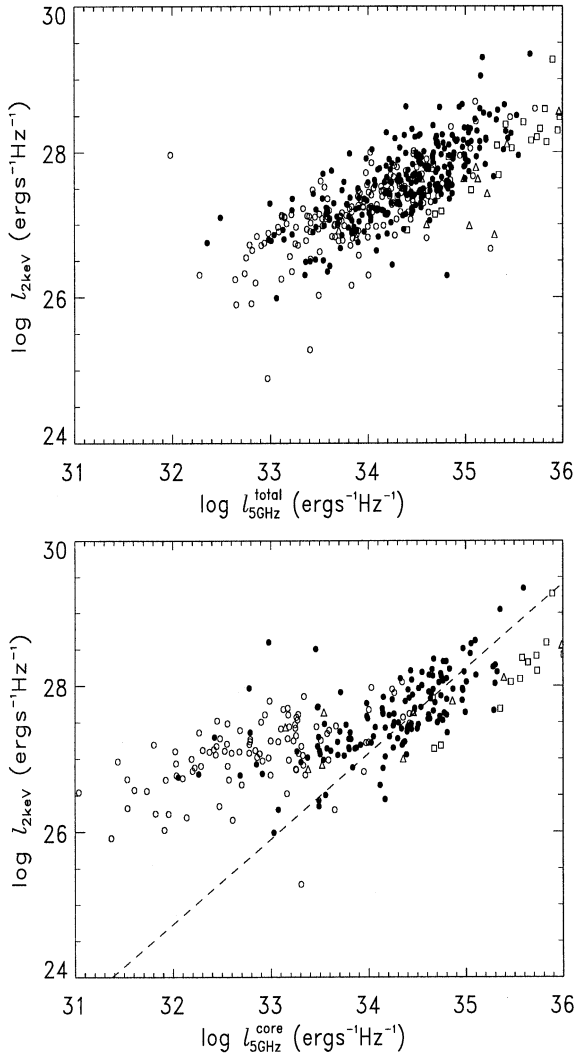

Fig. 13. The monochromatic X-ray luminosity as a function of the total 5 GHz luminosity (upper panel) and as a function of the 5 GHz core luminosity (lower panel). Open circles: steep spectrum quasars, dots: flat spectrum quasars. The linear regression line is for objects with core luminosities higher than log l_{core} = 34.2.

5.4. l_x- l_r- correlations

In Fig.13 we plot the monochromatic X-ray luminosity at 2 keV as function of the 5 GHz radio luminosity: in the upper panel the total radio luminosity is taken, in the bottom panel (for objects where these data are available) the core luminosity.

An ODR correlation analysis gives for the correlation of the X-ray luminosity with total radio luminosity a slope of β_{FS} = 0.73 ± 0.11 for flat spectrum sources and β_{SS} = 0.82 ± 0.13 for the steep spectrum sources. For the 5 GHz radio fluxes typical errors of $\sim 15\%$ are used. However, the results are not sensitive to the actual magnitude of the errors. Both slopes are consistent with each other within their 1 σ uncertainties, but flat spectrum sources are on average more luminous.

Separating the radio core and radio lobe components of a sample of 3CR quasars, Tananbaum et al. (1983) concluded that the X-ray flux is correlated with the core but not with the lobe radio flux. Later Kembhavi et al. (1986) confirmed the much tighter correlation between X-ray and radio core flux indicating that both emission processes are related and originate in the central regions of the objects. The correlation analysis for the X-ray versus core luminosity yielded for flat spectrum sources $\beta_{c,FS}$ = 0.68 ± 0.13 and for the steep spectrum sources $\beta_{c,SS}$ = 0.47 ± 0.14, again consistent with a single slope within the mutual 1 σ errors. We therefore fitted the whole sample with a single line and obtained a slope of $\beta_{tot} = 0.45 \pm 0.07$. However, the data (Fig. 13, bottom panel) seem to indicate a steepening of the slope towards higher luminosities ($l_{core} \geq 10^{34}$ erg s^{-1} Hz^{-1}). A fit of two lines with a break luminosity of log (l_r) $\sim$ 34.2 resulted in a flat slope of $\beta_l = 0.42 \pm 0.12$ at luminosities lower than the break luminosity, and of $\beta_h = 1.17 \pm 0.36$ at higher core luminosities. However, the reduced χ^2 of this fit is only marginally lower than the fit with a single line. We thus cannot confirm on a statistically sound basis a clear separation of steep spectrum and flat spectrum quasars as claimed by Baker et al. (1995) for a much smaller data set. However, Fig. 13 is indicative for the existence of two X-ray components, which can be interpreted in terms of two distinct components of the X-ray emission, an unbeamed and a beamed one correlated with l_{core} (Baker et al. 1995, Browne & Murphy 1987).

To test the relationship between radio morphology and X-ray luminosity we separated out the contribution from the flat spectrum cores to the X-ray luminosity, given by the fitted form at high R (see below, Table 4 and the dashed line in Fig. 15) log (l_x) = 0.97 (log (l_{core}) - 34) + 27.17. With this relation we estimated the core X-ray luminosity $l_{x,c}$. In Fig.14 we plot the logarithmic ratio log(l_x/$l_{x,c}$) as a function of the radio core dominance R for all objects with known radio core luminosity. This corresponds to the the excess values of log(l_x) above the extrapolated line for the core X-ray luminosity $l_{x,c}$. The ratio log(l_x/$l_{x,c}$) is found to anti-correlate strongly with R. The dashed line shows the predictions by the two component model of Kembhavi (1993) which are slightly different from those of Browne & Murphy (1987) (see Baker et al. 1995). However, both models contain some ad hoc assumptions which do not seem to hold in the light of our data.

Our sample is large enough to study subgroups characterized by suitably restricted radio parameters. We find that the measured value of the core flux (i.e., the core luminosity alone) is possibly not the physically dominating parameter. The radio core dominance, R, in connection with l_{core} seems to be more suited. Performing a regression analysis of $l_x \sim l_{core}^{\beta}$ in various ranges of the core dominance parameter we find that the slope of the regression curve steepens with R. In Table 4 we list the results of the analysis. Given are the core dominance parameters, the number of objects, and the slope of the correlation, determined by an ODR analysis.

There is a clear trend of a steepening of the slope with increasing core dominance. In Fig. 15 we show the obtained correlation for the objects with highest core dominance ($R > 10$, full dots) and for the objects with very low values of $R < 0.5$, (open circles). It is interesting to note, that the core luminosity

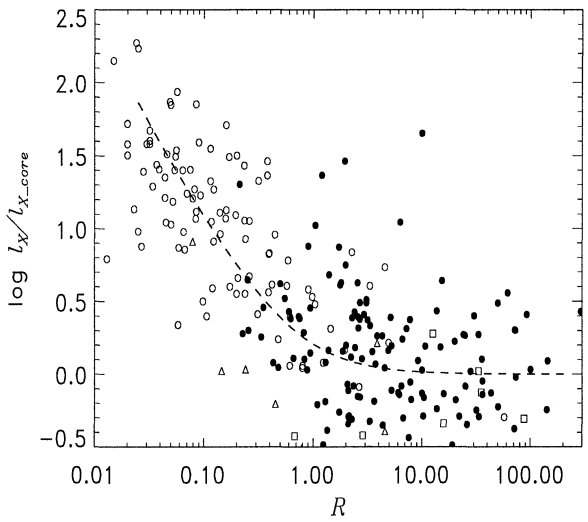

Fig. 14. Plot of the logarithmic ratio of total-to-core X-ray luminosities versus R. See text for details.

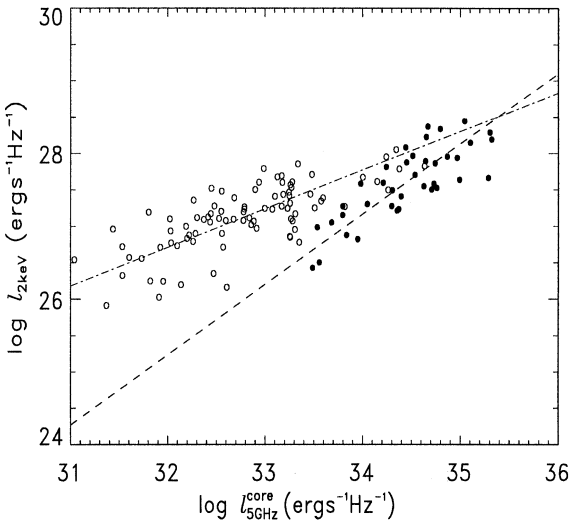

Fig. 15. The monochromatic X-ray luminosity as a function of the 5 GHz core luminosity. Full dots are objects with core dominance $R > 10$, open circles objects with $R < 0.5$.

Table 4. Regression analysis for various core dominances

Core dominance	N($> R$)	slope
R > 10	38	0.97$\pm$ 0.33
R > 5	57	0.86$\pm$ 0.24
R > 2	96	0.80$\pm$ 0.18
R < 0.5	87	0.53$\pm$ 0.14
R < 0.1	45	0.70$\pm$ 0.23

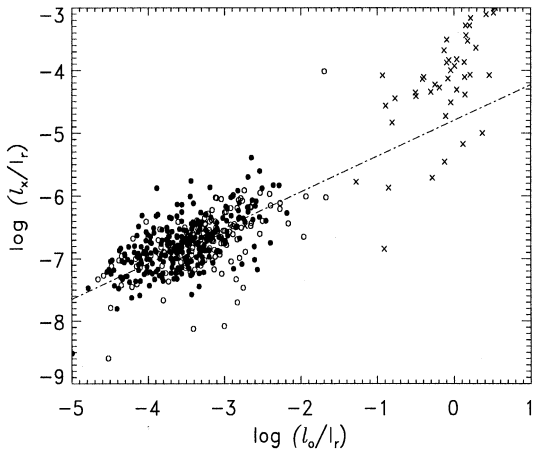

Fig. 16. Luminosity - ratios l_x/l_r versus l_o/l_r. The linear regression line for the steep and flat spectrum sources is plotted as dash-dotted line. The symbols have the usual meaning; crosses are the radio detected quasars not fulfilling the 'radio-loud' flux ratio criterion.

spans more than two orders of magnitudes even for the restricted ranges of R, which indicates large intrinsic differences in the power of the jets. And, even at lowest R-values, where the emission should be completely dominated by unbeamed emission, a strict correlation holds between l_x and l_{core}, showing that the unbeamed radio and X-ray components are as well correlated over a wide range of the intrinsic power of the cores.

Further, at a given core luminosity there is a clear tendency that objects with lower R - values show higher X-ray luminosities. From the definition of R this means that even the extended radio flux is positively correlated with the X-ray luminosity, however, with a different slope. Therefore, any simple correlation found between luminosities like $l_x \sim l_{core}^{\beta}$ must be questionable as other physically relevant parameters are neglected.

Finally, it should be noted that a similar analysis for a R - dependent l_x- $l_o$correlation does not reveal statistically significant deviations between the slopes of the correlations. This seems to imply that the optical and the X-ray emission are directly linked, i.e., the optical emission is partly beamed as well.

5.5. Redshift - independent quantities

Some of the correlations could be introduced by distance dependent luminosity selection through the inherent sensitivity limits of the different catalogues. Nearly distance independent correlation diagrams can be constructed by using flux or luminosity ratios. It must be noted, however, that the applied K-corrections still introduce different z-dependencies into the calculated luminosities and that the samples themselves are possibly subject to Malmquist biases.

In Fig. 16 we plot the ratios l_x/l_r versus l_o/l_r for the sample of both, radio-loud and radio-quiet sources for which 5 GHz fluxes are available. The flat spectrum and steep spectrum quasars populate a well defined, relatively narrow region in the diagram with an obvious correlation between the luminosity ratios. A regression analysis for the logarithmic luminosity ratios for flat and steep spectrum objects gives a slope of β_{fs+ss} = 0.57 $\pm$ 0.09 with a correlation coefficient of R_{sp} = 0.58 and a nearly 100% confidence level for the existence of a correlation. This

correlation between luminosity ratios for quasars would imply that we have a dependency of the form $l_x \sim {l_r}^{\alpha}\, {l_o}^{\beta}$, as claimed previously by Kembhavi et al. (1986), Worrall et al. (1987), and others. This further argues against a simple correlation of the form $l_x \sim l_o$ discussed above in Sect. 5.2.

The relatively narrow range of X-ray - to - radio flux ratios (less than two orders of magnitude) compared to the wider spread along the horizontal axis in Fig.16 argues for a closer link between these two radiation mechanisms than that for the X-ray and optical emission. The two objects with very large l_x/l_r ratios are PKS 0558-504 and OZ 453.7 which seem to be 'peculiar' in a general sense. They will be discussed in a subsequent paper, together with other extreme objects of the sample[2]. Interestingly, the objects with very low radio fluxes, not qualifying as radio-loud quasars are close (but slightly above) the extrapolation of the regression line of the radio-loud objects. They are characterized by a diminishing influence of the radio emission properties and might follow a simple $l_x \sim l_o$ correlation which will be discussed in more detail by Yuan et al. (1996).

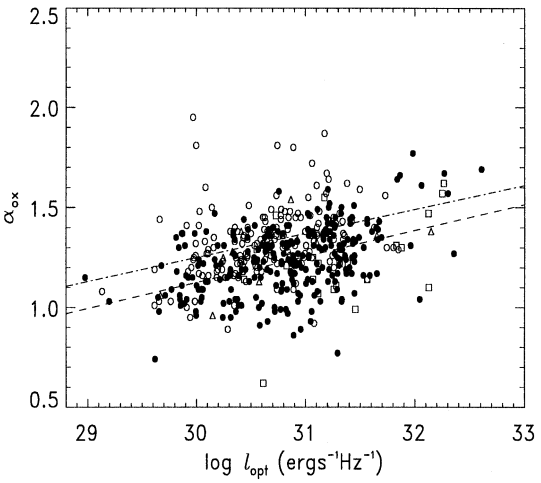

Fig. 17. X-ray loudness α_{ox} versus optical luminosity. The full line is the regression slope for steep spectrum objects, the dashed line that for flat spectrum quasars.

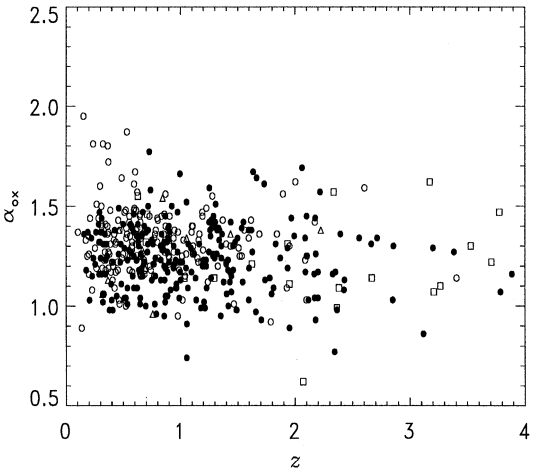

Fig. 18. X-ray loudness α_{ox} versus redshift z.

6. Broad band spectral evolution

The emission from quasars appears to be 'scale-free': from the lowest to the highest luminosities the quasar continuum and emission lines scale almost linearly with luminosity and are independent of redshift (Blandford 1990). The fraction of the power emitted in the different energy bands remains similar, although a slowly decreasing X-ray loudness has been found for higher luminosity quasars (Worrall et al. 1987). However, an exact quantitative assessment seems to be difficult due to selection biases and apparent changes in the source population at different redshifts.

The X-ray loudness $\alpha_{ox} = -0.384\ log\ (l_{2\ keV}/l_{2500\text{Å}})$ has been used frequently in the past for the discussion of the relative fraction of X-ray to optical emission in an evolving quasar source population. In Fig. 17 we show a plot of α_{ox} versus optical luminosity. A regression analysis yields $\alpha_{ox,s} = (0.123 \pm 0.024)(log\ l_o - 30.5) + (1.309 \pm 0.012)$ for the steep spectrum sources while for flat spectrum sources we get $\alpha_{ox,f} = (0.130 \pm 0.016)(log\ l_o - 30.5) + (1.193 \pm 0.011)$. In both cases the probability levels for a correlation are $P_r < 10^{-8}$. The two slopes are consistent with each other in their mutual 1 σ errors but the larger value of the regression constant for flat spectrum quasars shows that, in agreement with the results of Sect. 5.2, flat spectrum quasars are X-ray louder than the steep spectrum objects. Similar slopes have been found for the optically selected LBQS quasars (Green et al. 1995) and from Einstein data with different analysis techniques by Avni & Tananbaum (1986), Wilkes et al. (1994), and Avni et al. (1995).

However, a slope of $\beta \sim 0.11$ implies a non-linear relation $l_x \sim l_o^{0.7}$, inconsistent with the value of ~ 1 found in chapter 5 (see the discussion).

Again, it cannot be ruled out that this correlation is introduced by a redshift dependence of the luminosities and in fact, Fig. 18 indicates there might be a redshift dependence of the X-ray loudness. We obtain fits of the form $\alpha_{ox,fs} = (1.26 \pm 0.02) - (0.02 \pm 0.02) \times z$ for the flat spectrum objects and $\alpha_{ox,ss} = (1.36 \pm 0.02) - (0.04 \pm 0.02) \times z$ for steep spectrum sources, however both with relatively large probability levels of $P_r = 0.32$ and $P_r = 0.35$, respectively and thus a strong redshift dependence cannot be confirmed. Correspondingly, for simple redshift independent averages we get $< \alpha_{ox} >_{fs} = 1.24 \pm 0.01$, $< \alpha_{ox} >_{ss} = 1.33 \pm 0.01$, $< \alpha_{ox} >_{GPS} = 1.24 \pm 0.05$, and $< \alpha_{ox} >_{CSS} = 1.27 \pm 0.05$

These values are in good agreement with those found in previous studies considering the generally large errors of smaller samples. They seem to be considerably smaller than those for radio quiet quasars found by Green et al. (1995), demonstrating that radio-quiet quasars are less X-ray bright at a given optical

[2] There might be more than one X-ray source in the ROSAT error box contributing to the X-ray flux attributed to OZ 453.7.

luminosity. But it must be noted that the different selection criteria of the two samples makes it hard to compare them directly.

7. Discussion

The large sample of radio-loud quasars available from ROSAT observations allowed a detailed study of the spectral X-ray properties of various subsamples, the correlations between X-ray and radio properties, as well as the broad band energy distribution of the objects. For the statistical analyses we used the restricted sample of radio selected quasars only. However, the corresponding results from the whole sample of all radio-loud quasars are only slightly different in their numerical values (all inside the mutual 1σ errors) and show the same general trends. This means that the inclusion of originally optically or X-ray selected quasars does not lead to detection biases.

In Sect. 4.1 we showed that the power law indices of the soft X-ray spectra differ for the various radio classes of quasars, with steep spectrum sources having a steeper slope than the flat spectrum quasars. However, the correlation of X-ray spectral index with redshift indicates that at redshift zero both classes have similarly steep soft X-ray spectra. As the spectral slopes for steep spectrum sources flatten considerably less with redshift, their average power law index appears to be steeper for a large sample of objects. The correlations of X-ray spectral index with redshift strongly suggests that radio-loud quasars have two spectral components: a flat power law at higher energies, which is related to the radio core emission and an additional steeper component in the ROSAT energy band. At z = 0 the soft X-ray spectra are dominated by the steep component, and flat and steep spectrum sources have similar indices. With increasing z this steep component moves out of the PSPC's energy band and the X-ray spectrum is a combination of the two components. The generally flatter soft X-ray power law spectra can then be attributed to a more dominant flat X-ray component in flat spectrum radio sources - a scenario which also accounts for the fact that flat spectrum radio sources are X-ray louder than their steep spectrum counterparts. The flat component can be recognized in Fig. 6 for the flat spectrum quasars but, unfortunately, there are no data available for steep spectrum quasars at higher redshifts. If the flat power law component is related to beamed emission from the core and the steeper low energy component with an isotropic unbeamed component (Browne & Murphy 1987), the above results are in accordance with current unification schemes which attribute the different classes of objects to different viewing conditions (Barthel 1989).

Similar ideas have been followed by Jackson et al. (1993) to explain the different spectral slopes generally found for AGN in the ROSAT and in the wider Einstein IPC energy band. Whereas the steeper ROSAT spectra could be reproduced the simulated Einstein spectra were too steep. However, as Bühler et al. (1994) showed recently, these results strongly depend on the parameterization of the soft component in these models.

However, the above simple two component interpretation is not quite consistent with expectations of these schemes: in that framework one would expect that the X-ray emission from radio galaxies is predominantly the unbeamed, isotropic component with steep spectral slope. But the average X-ray slope found for radio galaxies (Papers I, II) is around $< \Gamma > \sim 1.8$.

Another important issue in that respect is the relation between the X-ray spectral properties and the radio properties of the objects. We found correlations between the power law photon index Γ and the radio spectral slope α_r, the radio loudness R_L, and the core dominance R. These parameters themselves are, to a high degree, interrelated and indicators for orientation effects (for example, the radio spectral index can directly be related to the core dominance parameter). They further depend, at least via selection effects, on the redshift z as well and it remains unclear which physically dominating parameter is accounting for the correlations. Again, viewing conditions might be responsible - at least in the extreme cases of flat spectrum and steep spectrum objects. In most correlations the transition between these two object classes is rather abrupt.

A final question related to the X-ray spectral properties is that of a possible correlation of the amount of absorption towards a source with its distance (redshift). There seems to be no additional absorption increasing with redshift, at least up to $z \sim 2$. However, we cannot answer this question with any reliable statistical significance as the quality of the spectra is relatively poor for most of the distant sources and there is substantial scatter in the data. This scatter seems to be related to individual sources, i.e., some objects (especially at higher redshifts) show additional absorption associated with the quasar itself. Further, there is growing evidence that this extra absorption is not a 'fixed' property of a particular object but that the intrinsic absorption can vary strongly with time (Comastri et al. 1996, Schartel et al. 1996).

Correlations between the emission at different wavelengths are indicators for the underlying emission processes. A vast number of papers addressed this question - with differing results. The quoted reasons for these discrepancies range from the definitions of the samples studied to the mathematical methods applied in the analysis. We have shown how the latter influence the luminosity correlations in our sample and came to the conclusion that methods taking into account errors in both variables were the most appropriate ones.

Even with these techniques the slopes of the l_x- l_r- correlations were less than unity, that for the l_x- l_o- correlations could be consistent with a slope of unity, expected from the study of the luminosity functions. However, the correlations involving the radio luminosities clearly show that there are higher order effects in the data and that a single straight line very likely does not represent the true physical connection between the variables.

Our analysis in Sect. 5.4 indicates that the observed X-ray luminosity depends on the total intrinsic radio power of the quasar and, additionally, on the amount of beaming in the source. Assuming that the observed total X-ray luminosity is composed of two contributions, one related to the radio core luminosity, one to the extended emission, i.e., $\log(l_x) = \beta_1 \log(l_{core}) + \beta_2 \log(l_{ext}) + \text{const}$, and using the fitted slopes for high R and low R objects from Sect. 5.4 the representation of the X-ray data with this model results in a largely improved χ^2 value

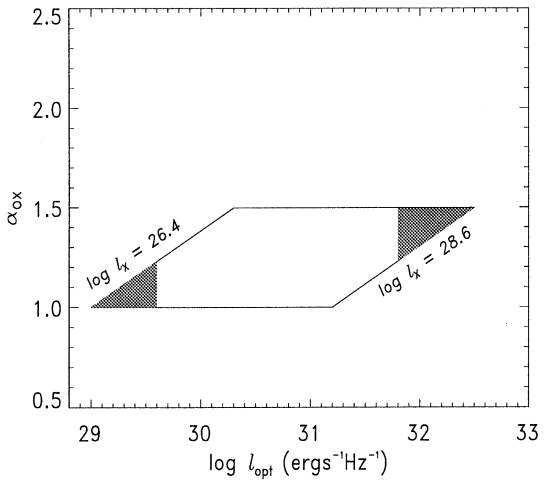

Fig. 19. Phase space of the X-ray loudness α_{ox} versus optical luminosity of a sample of objects with limits on the X-ray luminosity as found for the current quasar sample. Shaded areas denote phase space regions devoid of sources (see Fig. 15).

compared to the fits of l_x versus l_{core} or versus l_{tot}. This strongly indicates that the two-component model is a better description of the physical situation in the objects.

It must further be noted, that the set of parameters for the correlations found between the various luminosities and their ratios is not self consistent. The reasons are either, that some (or all) of the correlations are not linear, that there is a strong redshift or selection dependency in the data, or that the considered subclasses of objects are exhibiting different luminosity dependencies.

Some correlations, like that of the X-ray luminosity versus core dominance or X-ray loudness versus core dominance can be traced back directly to the different emission properties of the flat and steep spectrum sources. We do not find correlations of broad band spectral properties α_{ox}, α_{ro}, or α_{rx} with redshift z, however, these quantities seem to correlate with the luminosities.

One of the most discussed correlations is that of the X-ray loudness α_{ox} versus optical luminosity l_o (Kriss & Canizares 1985, Pickering et al. 1994, Green et al. 1995, Avni et al. 1995). The slope of ~ 0.12 found in chapter 6 (similar values are obtained in the other papers as well) is inconsistent with a slope of unity in the log(l_x) - log(l_o) correlation and various physical explanations can be found for the apparent inconsistencies (Pickering et al. 1994, Della Ceca et al. 1994).

Taking the slope determined for the α_{ox} - l_o dependence, we fail to find the expected α_{ox} - l_x correlation in our data. Therefore, we believe that at least a major fraction of the claimed correlation is caused by selection effects. Assuming a constant α_{ox} with a certain dispersion σ as well as upper and lower luminosity limits for the X-ray data the sources should occupy a phase space region as depicted in Fig. 19.

With a Monte-Carlo simulation we 'filled' the rhomboid with the same number of test particles as data points in Fig. 17 with various constant values for α_{ox} and dispersion σ_α.We then performed regression analyses on these data as above. With α_{ox} = 1.27 and a dispersion σ_α = 0.17 we obtained the same slope of ~ 0.12 found in chapter 7.

In addition to luminosity boundaries for l_x we see optical luminosity boundaries in the data: there are hardly any data below log(l_o) = 29.6 and above log(l_o) = 31.8. These regions correspond to the shaded regions in Fig. 19. Taking into account these limits in the Monte-Carlo simulations we obtain the above fitted slope with a dispersion of σ_α = 0.17 and the same constant value for α_{ox}.

Thus we conclude that the claimed correlation between α_{ox} and l_o is mainly caused by luminosity selection effects in conjunction with the intrinsic dispersion of the α_{ox} distribution (similar arguments hold for the α_{rx} - l_r and the α_{ro} - l_r correlation) and that a linear correlation between log(l_x) and log(l_o) might quite well hold. There are, however, indications for a lack of very X-ray luminous quasars at very high optical luminosities in the data and we can certainly not rule out a non-linear correlation or correlations of higher order.

8. Conclusions

We have presented the broad band properties of the largest sample of X-ray detected radio-loud quasars published so far. The large number of objects allowed the study of the class specific properties of these objects with high statistical significance.

We found correlations between the luminosities and the spectral properties which are often related to some general class properties of the objects, like the radio spectral index. For example, flat spectrum quasars are X-ray louder than steep spectrum objects. Although most of these correlations could be confirmed with formally very small errors and high statistical significances it is not always certain whether these correlations are genuine, caused by flux limitations of the underlying databases, or induced by a physically different, hidden, and not yet understood parameter. Especially the spectral properties (flat/steep radio spectrum, CSS, GPS) and the correspondingly derived parameters (radio loudness, core dominance) seem to be interrelated with the redshift z which introduces detection biases through luminosity K-corrections.

Most of the correlations found can be reconciled in the framework of viewing dependent emission in all frequency bands, however, a quantitative analysis still remains to be done. The X-ray, the radio, and eventually even the optical emission seems to consist of two separate components, an isotropic one with steep spectra and a 'beamed' component with a flat spectrum. Whether this beaming is only a viewing angle effect or whether it includes additional Doppler boosting remains unclear.

Some questions remain open, for example the high detection rate of high z quasars and the lack of optically very bright, X-ray luminous sources. Whereas the small number of CSS sources appears to be inconspicuous in all correlations, perhaps with slightly higher ratios of radio- to X-ray and radio- to optical

luminosities, the GPS objects are predominantly found at higher redshifts with high radio and X-ray luminosities.

Even pure selection effects might be important as we are discussing catalogued, previously identified objects only, which were often found due to some unusual or outstanding observational properties.

Finally we want to mention that ROSAT's soft energy band can introduce biases as well, as the emission of the spectral region of the blue bump moves out of the PSPC's energy window with increasing redshift.

Acknowledgements. The ROSAT project is supported by the Bundesministerium für Bildung, Wissenschaft, Forschung und Technologie (BMBF) and the Max-Planck-Gesellschaft. We thank W. Voges for supplying data from the newest reprocessing of the RASS and our colleagues from the ROSAT group for their support, M. Véron-Cetty for supplying a machine readable form of their catalogue, and J. Baker and E. Feigelson for communicating radio core fluxes. We thank the referee, P. Véron, for many useful comments for the improvement of the manuscript. This research has made use of the NASA/IPAC Extragalactic Data Base (NED) which is operated by the Jet Propulsion Laboratory, California Institute of Technology, under contract with the National Aeronautics and Space Administration.

References

Avni Y., Tananbaum H., 1986, ApJ 305, 83
Avni Y., Worrall D.M., Morgan, Jr. W.A., 1995, ApJ 454, 673
Baker J.C., Hunstead R.W., 1995, ApJ 452, L95
Baker J.C., Hunstead R.W., Kapahi V.K., Subrahmanya C.R., 1994, in: The Physics of AGN, Bicknell G.V., Dopita M.A., Quinn P.J. (eds), ASP Conference Series Vol. 54, San Francisco, p. 195
Baker J.C., Hunstead R.W., Brinkmann W., 1995, MNRAS 277, 553
Bechtold J., Elvis M., Fiore F., et al., 1994, AJ 108, 759
Blandford R.D., 1990, in: 'Active Galactic Nuclei', T.J.-L. Courvoisier, M. Mayors (eds), Saas-Fee Advanced Course 20, Springer Verlag, Berlin, p.161
Barthel P.D., 1989, ApJ 336, 319
Boggs P.T., Byrd R.H., Schnabel R.B., 1987, SIAM J. Sci. Stat. Comput. 8, 1052
Bolton J.G., Wright A.E., Savage A., 1979, Aust. J. Phys., Astrophys. Suppl., No. 46, 1
Boyle B.J., Griffiths R.E., Shanks T., Stewart G.C., Georgantopoulos I., 1993, MNRAS 260, 49
Brinkmann W., 1992, in: Proc. of the Conference *X-ray Emission from AGN and the Cosmic X-ray Background*, MPE Report 235, p. 143
Brinkmann W., Siebert, J., Boller, Th., 1994, A&A 281, 355 (Paper I)
Brinkmann W., Siebert, J., Reich W., et al, 1995, A&AS 109, 147 (Paper II)
Browne I.W.A., Murphy D.W., 1987, MNRAS 226, 601
Brunner H., Worrall D.M., Wilkes B.J., Elvis M., 1989, in: Proc. 23rd ESLAB Symposium (ESA SP-296), Noordwijk, ESA, p.905
Brunner H., Friedrich P., Zimmermann H.-U., Staubert R., 1992, in: Proc. of the Conference *X-ray Emission from AGN and the Cosmic X-ray Background*, MPE Report 235, p. 198
Brunner H., Lamer G., Staubert R., Worrall D. M., 1994, A&A 287, 436
Bühler P., Courvoisier T. J. L., Staubert R., 1994, A&A 287, 433
Bühler P., Courvoisier T. J. L., Staubert R., et al., 1995, A&A 295, 309
Canizares C.R., White J.L., 1989, ApJ 339, 27
Cappi M., Matsuoka M., Comastri A., et al., 1996, subm. to ApJ
Cheng F.Z., Danese L., DeZotti G., Lucchin F., 1984, MNRAS 208, 799
Comastri A., Cappi M., Matsuoka M., 1996, in: Proc. of the Conference *X-rays from the Universe*, MPE Report 263, in press.
Della Ceca R., Zamorani G., Maccacaro T., et al, 1994, ApJ 430, 533
Draper N.R., Smith, H., Applied Regression Analysis, John Wiley, New York, 1966
Elvis M., Fiore F., Wilkes B., McDowell J., Bechtold J., 1994, ApJ 422, 60
Elvis M., 1994, in: F. Makino, T. Ohashi (eds), New Horizon of X-Ray Astronomy, Univ. Acad. Press, Tokyo, p. 323
Elvis M., 1996, in: Proc. of the Conference *X-rays from the Universe*, MPE Report 263, in press.
Fasano G., Vio R., 1988, Newsletter of the Working Group for "Modern Astronomical Methodology", 7, 2
Fanti R., Fanti C., Schilizzi R.T., et al., 1990, A&A 231, 333
Fanti C., Fanti R., 1994, in: The Physics of AGN, Bicknell G.V., Dopita M.A., Quinn P.J. (eds), ASP Conference Series Vol. 54, San Francisco, p. 341
Feigelson E.D., Berg C.J., 1983, ApJ 269, 400
Feigelson E.D., Babu G.J., 1992, ApJ 397, 55
Franceschini A., La Franca F., Cristiani S., Mirones J.M., 1994, MNRAS 269, 683
Gower J.F.R., Scott P.F., Wills D., 1967, Mem. Roy. Astron. Soc. 71, 49
Grueff G., Vigotti M., 1975, A&AS 20, 57
Green P.J., Schartel N., Anderson S.F., et al., 1995, ApJ 450, 51
Jackson N., Browne I.W.A., Warwick R.S., 1993, A&A 274, 79
Kembhavi A., 1993, MNRAS 264, 683
Kembhavi A., Feigelson E.D., Singh K.P., 1986, MNRAS 220, 51
Kriss G.A., Canizares C.R., 1985, ApJ 297, 177
Kühr H., Witzel A., Pauliny-Toth I.I.K., Nauber U., 1981a, A&AS 45, 367
Kühr H., Witzel A., Schmidt J., 1981b, AJ 86, 854
La Franca F., Franceschini A., Cristiani S., Vio R., 1995, A&A 299, 19
Laing R.A., Riley J.M., Longair M.S., MNRAS 204, 151
Laor A., Fiore F., Elvis M., Wilkes B., McDowell J.C., 1994, ApJ 435, 611
Large M.I., Mills B.Y., Little A.G., Crawford D.F., Sutton J.M., 1981, MNRAS 194, 693
Laurent-Muehleisen S.A., Kollgaard R.I., Ryan P.J., et al., 1996, A&AS in press
LaValley M., Isobe T., Feigelson E.D., 1992, In: Astronomical Data Analysis Software and Systems, eds. D.M. Worrall, C. Biemesderfer, J. Barnes, San Francisco: ASP Conf. Series Vol. 25, p.245
Lawson A.J., Turner M.J.L., Williams O.R., Stewart G.C., Saxton R.D., 1992, MNRAS 259, 743
Maccacaro T., Gioia I. M., Wolter A., Zamorani G., Stocke J., 1988, ApJ 326, 680
Neumann M., Reich W., Fürst E., et al., 1994, A&AS 106, 303
O'Dea C.P., Baum S.A., Stanghellini C., 1991, ApJ 380, 66
Padovani P., 1992, A&A 256, 399
Pauliny-Toth I.I.K., Witzel A., Preuss E., et al., 1978, AJ 83, 451
Pickering T.E., Impey C.D., Foltz C.B., 1994, AJ 108, 1542
Press W.H., Flannery B.P., Teukolsky S.A., Vetterling W.T., 1986, Numerical Recipes, Cambridge Univ. Press, 488
Schartel N., Fink H., Brinkmann W., Trümper J., 1992, in: Proc. of the Conference *X-ray Emission from AGN and the Cosmic X-ray Background*, MPE Report 235, p. 195

Schartel N., 1995, PhD thesis, University of München
Schartel N., Brinkmann W., Fink H.H., Trümper J., Wamsteker W., 1996, A&A submitted
Schartel N., Walter R., Fink H.H., Trümper J., 1996, A&A 307, 33
Schmidt M., Green R.F., 1986, ApJ 305, 68
Shastri P., Wilkes B.J., Elvis M., McDowell J., 1993, ApJ 410, 29
Siebert J., Matsuoka M., Brinkmann W., Cappi M., Mihara T., Takahashi T., 1996, A&A 307, 8
Stocke J.T., Morris S.L., Weynmann R.J., Foltz C.B., 1992, ApJ 396, 487
Tananbaum H., Wardle J.F.C., Zamorani G., Avni Y., 1983, ApJ 268, 60
Veron-Cetty M.-P., Veron P., 1993, A Catalogue of Quasars and Active Nuclei (6th Edition), ESO Scientific Report No. 13 (VV93)
Voges W., 1992, In: Proc. of the ISY Conference "Space Science", ESA ISY-3, ESA Publications, p.9
Voges W., Gruber R., Paul J., et al., 1992, In: Proc. of the ISY Conference "Space Science", ESA ISY-3, ESA Publications, p.223
Voges W., Gruber R., Haberl F., et al., 1995, ROSAT NEWS No. 32
Wilkes B.J., Elvis M., 1987, ApJ 323, 243
Wilkes B.J., 1994, in: The Physics of AGN, Bicknell G.V., Dopita M.A., Quinn P.J. (eds), ASP Conference Series Vol. 54, San Francisco, p. 41
Wilkes B.J., Tananbaum H., Worrall D., et al., 1994, ApJ Suppl 92, 53
Williams O.R., Turner M.J.L., Stewart G.C., et al., 1992, ApJ 389, 157
Wills B.J., Brotherton M.S., 1995, ApJ 448, L81
Worrall D.M., Giommi P., Tananbaum H., Zamorani G., 1987, ApJ 313, 596
Worral D.M., Wilkes B.J., 1990, ApJ 360, 396
Yuan W., Brinkmann W., 1996, in preparation
Zhang Y. F., Marscher A. P., 1994, in: The soft X-ray cosmos, Schlegel E. M., Petre R., (eds), AIP Conf. Proc. 313, AIP, New York, p.406

This article was processed by the author using Springer-Verlag LaTeX A&A style file *L-AA* version 3.